



# How to Read and Determine the Specific Surface Area of Inorganic Materials using the Brunauer-Emmett-Teller (BET) Method

Ferli Septi Irwansyah<sup>1,2\*</sup>, Alfi Ikhlusal Amal<sup>3</sup>, Erlinda Widyasmara Diyanthi<sup>3</sup>, Eko Prabowo Hadisantoso<sup>3</sup>, Atiek Rostika Noviyanti<sup>1</sup>, Diana Rakhmawaty Eddy<sup>1</sup>, Risdiana Risdiana<sup>4</sup>

<sup>1</sup>Departement of Chemistry, Faculty of Mathematics and Natural Sciences, Universitas Padjadjaran, Indonesia

<sup>2</sup>Departement of Chemistry Education, UIN Sunan Gunung Djati Bandung, Indonesia

<sup>3</sup>Departement of Chemistry, UIN Sunan Gunung Djati Bandung, Indonesia

<sup>4</sup>Departement of Physics, Faculty of Mathematics and Natural Sciences, Universitas Padjadjaran, Indonesia

\*Correspondence: E-mail: [ferli@uinsgd.ac.id](mailto:ferli@uinsgd.ac.id)

## ABSTRACT

The specific surface area of inorganic materials is a crucial parameter that influences their performance in various applications. The Brunauer-Emmett-Teller (BET) method is widely used for accurately determining the surface area of porous materials. This study presents a comprehensive guide to determining the specific surface area of inorganic materials using the BET method. The paper outlines the theoretical background of the BET method, the experimental procedures involved, and the data analysis techniques. Additionally, we discuss the limitations and potential sources of errors in the BET method. The proposed guide aims to provide researchers and practitioners with a systematic approach to accurately measure the specific surface area of inorganic materials, enabling informed decision-making and enhancing material design and optimization processes.

## ARTICLE INFO

### Article History:

Submitted/Received 28 Apr 2023

First Revised 05 May 2023

Accepted 23 Jul 2023

First Available online 24 Jul 2023

Publication Date 01 Mar 2024

### Keyword:

BET method,

Surface area analyzer,

SAA,

Brunauer-emmett-teller method,

Inorganic materials.

## 1. INTRODUCTION

The Brunauer-Emmett-Teller (BET) method is a fundamental technique used to measure the specific surface area of porous materials, such as solids and powders. Surface area is important, especially facing materials with porous structures. This analysis has been used in many researches relating to adsorption process (Ragadhita & Nandiyanto, 2021; Nandiyanto *et al.*, 2023a; Nandiyanto *et al.*, 2023b; Mutolib *et al.*, 2023; Ragadhita *et al.*, 2023; Nandiyanto *et al.*, 2022a; Nandiyanto *et al.*, 2022b; Nandiyanto *et al.*, 2023c; Nandiyanto *et al.*, 2023d; Nandiyanto *et al.*, 2022c; Nandiyanto *et al.*, 2022d; Nandiyanto *et al.*, 2023e).

It is named after the three scientists who developed it: Stephen Brunauer, Paul Hugh Emmett, and Edward Teller. The method was first introduced in 1938 in their seminal paper titled "Adsorption of Gases in Multimolecular Layers" (Brunauer *et al.*, 1938).

The specific surface area of a material is a crucial property that influences its behavior in various applications, including catalysis, gas adsorption, and chemical reactions. The BET method is widely employed in scientific research, industrial processes, and quality control to determine the surface area of materials with high accuracy and reproducibility (Yang *et al.*, 2023).

The principle behind the BET method is based on the adsorption of gas molecules onto the material's surface. When gas is exposed to a solid, it adheres to the surface due to attractive forces, forming a layer of adsorbed molecules. As the pressure of the gas increases, additional layers are formed, leading to a multilayer adsorption phenomenon (Nasrollahzadeh *et al.*, 2019). The BET method assumes that gas molecules form a uniform layer on the surface, and the adsorption occurs in a monolayer fashion. It also assumes that the molecules do not interact with each other once they are adsorbed on the surface.

The process begins by exposing the solid material to a gas at a known temperature. The gas pressure is increased step by step, and the amount of gas adsorbed at each pressure is measured. These data are then used to plot the BET isotherm, a graph of the amount of adsorbed gas (typically nitrogen) against the relative pressure. The BET isotherm displays characteristic shapes, and the linear region at intermediate pressures is utilized for analysis (Thomas, 2023).

The BET method provides a means to calculate the monolayer capacity of the gas adsorbed on the material's surface, and from there, the specific surface area of the material can be determined. The monolayer capacity can be obtained by extrapolating the linear portion of the BET isotherm to zero relative pressure. The specific surface area is then calculated from the monolayer capacity, the molecular cross-sectional area of the gas, and a constant related to the energy of adsorption.

In summary, the Brunauer-Emmett-Teller method is a valuable tool for characterizing the surface area of porous materials. It plays a crucial role in understanding their properties and applications in various fields, including chemistry, materials science, and engineering (Shimizu & Matubayasi, 2022).

## 2. CURRENT THEORIES FOR BET METHOD

The Brunauer-Emmett-Teller (BET) method remains a widely accepted and reliable technique for determining the specific surface area of porous materials. There haven't been any radical changes in the underlying principles or theories of the BET method since its initial development. However, ongoing research and advancements in materials science and analytical techniques might lead to refinements or modifications in how the method is applied.

According to [Odler \(2003\)](#), there is some areas of interest and current research related to the BET method and surface area determination, including:

- (i) **Nanomaterials and Nanoporous Materials:** As nanotechnology advances, there is a growing interest in characterizing nanomaterials and nanoporous materials using BET and other complementary techniques. Researchers are exploring how the BET method can be applied to study the unique properties of nanomaterials and the effects of their small particle size on surface area determination.
- (ii) **High-Pressure Adsorption:** Traditional BET measurements are typically performed at relatively low gas pressures. However, there is an interest in expanding the application of BET to high-pressure gas adsorption, as it can provide valuable information about the porosity and surface area of materials under more realistic operating conditions
- (iii) **Non-Ideal Adsorption Behavior:** Some materials may exhibit non-ideal adsorption behavior, which can complicate the interpretation of BET data. Research is ongoing to develop models and methodologies to address such cases and improve the accuracy of surface area measurements.
- (iv) **Multicomponent Adsorption:** The BET method was originally developed for single-component gas adsorption. Researchers are exploring ways to extend the method for multicomponent gas adsorption, which is more representative of real-world scenarios.
- (v) **BET and Beyond:** While the BET method is widely used, it is not the only technique for determining surface area. Other methods, such as the Langmuir method, t-plot, and various gas adsorption methods, offer alternative approaches to characterizing porous materials. Researchers continually compare and improve these techniques to enhance accuracy and broaden their applicability.

It's important to note that the fundamental principles of the BET method have proven to be robust and accurate for many decades, and the method remains a standard tool for surface area characterization. As with any scientific field, ongoing research and technological advancements may lead to minor refinements or extensions of the method. However, the core principles continue to be the foundation of surface area determination using the BET method.

### 3. EXPERIMENTAL METHOD

To understand how to determine the specific surface area using the BET method, inorganic materials must first be characterized using the SAA (Surface Area Analyzer) instrument. The SAA instrument allows for the adsorption isotherm measurement, which is a crucial step in the BET method. Using the Surface Area Analyzer (SAA) instrument in The Brunauer-Emmett-Teller (BET) method is a crucial step in determining the surface area of porous materials. The process begins with sample preparation, where the porous material must be thoroughly cleaned and degassed to remove contaminants or adsorbed gases. Once the sample is ready, it is placed into the sample chamber of the SAA instrument. The instrument's setup involves connecting gas supply lines and vacuum connections per the manufacturer's guidelines. The instrument should be calibrated using standard reference materials with known surface areas to ensure accurate measurements if necessary.

The next stage involves the adsorption isotherm measurement. Nitrogen gas (N<sub>2</sub>) is commonly used as the adsorbate in the BET method due to its inert nature and well-defined adsorption behavior. Nitrogen gas is introduced into the sample chamber in incremental amounts at various relative pressures ( $P/P_0$ ). The instrument continuously records the amount of nitrogen gas adsorbed at each pressure step, resulting in data points that form the

adsorption isotherm. During this process, it is essential to allow the sample to reach equilibrium at each pressure step to ensure accurate measurements (Kruk et al., 1997).

Once the adsorption data is collected, the analysis calculates the surface area using the BET equation and relevant mathematical models. The isotherm data determines the monolayer adsorption capacity and specific surface area of the porous material. If a complete BET analysis is required, desorption measurements can be performed by reducing the pressure and measuring the amount of gas desorbed from the sample.

## 4. RESULTS AND DISCUSSION

### 4.1. Step-by-step analysis procedure bet method

Eight primary steps must be done in the analysis procedure to determine the specific surface area of a porous material, including:

- (i) Step 1: Sample Preparation. Grind the porous material to ensure a uniform particle size distribution and remove agglomerates. Thoroughly clean the sample to eliminate contaminants or adsorbed gases from the surface. Ensure the sample is dry and moisture-free, as water vapor could interfere with the adsorption measurements.
- (ii) Step 2: Degassing. Before the analysis, the sample must be degassed to remove any adsorbed gases or moisture. This step is critical to achieving accurate results. Place the sample in a vacuum oven and heat it under vacuum at an elevated temperature (typically 100-200°C) for several hours to remove any adsorbed gases or moisture.
- (iii) Step 3: Adsorption Measurements. Choose a suitable gas for the adsorption measurement. Nitrogen gas is commonly used due to its availability, inert nature, and ability to form a monolayer on most surfaces. Set up the adsorption apparatus, such as a gas adsorption analyzer or BET analyzer, and ensure it is properly calibrated. Introduce the degassed sample into the analysis chamber and equate it to the desired temperature.
- (iv) Step 4: BET Isotherm Data Collection. Begin the adsorption measurement by gradually increasing the pressure of the adsorbing gas while measuring the amount of gas adsorbed at each pressure step. The amount of gas adsorbed at each pressure point is typically determined by measuring the volume of gas taken up by the sample or changes in the gas pressure in the analysis chamber.
- (v) Step 5: Plotting the BET Isotherm. Plot the adsorbed gas quantity (usually in micromoles) against the relative pressure ( $P/P_0$ ), where  $P$  is the equilibrium pressure, and  $P_0$  is the saturated vapor pressure of the adsorbing gas. The BET isotherm will exhibit characteristic shapes. The region of interest for analysis is typically the linear portion of the isotherm, which occurs at intermediate relative pressures.
- (vi) Step 6: Linear Regression Analysis. Perform a linear regression analysis on the linear portion of the BET isotherm. The slope of the regression line provides the BET constant,  $C$ , which is related to the monolayer capacity of the adsorbed gas on the sample surface.
- (vii) Step 7: Calculation of Specific Surface Area. The BET equation can be represented in Equation (1) in terms of the specific surface area ( $S_{BET}$ ) and monolayer adsorption volume ( $V_m$ ).

$$\frac{P}{V_{ads}(P_0-P)} = \frac{1}{V_m C_B} + \frac{C_B-1}{V_m C_B} \left( \frac{P}{P_0} \right) \quad (1)$$

In Equation (1),  $V_{ads}$  denotes the volume of adsorbed  $N_2$  gas,  $C_B$  represents the constant, and  $P_0$  and  $P$  signify the saturated and equilibrium vapor pressure of  $N_2$  gas. The BET surface area ( $S_{BET}$ ) can be computed using the relationship given in Equation (2).

$$S_{\text{BET}} = 4.355 \times V_m \quad (2)$$

(viii) Verification and Interpretation. This step includes: (1) Validating the results and ensuring they are consistent with the material's physical properties, and (2) Interpreting the obtained specific surface area value in the context of the material's application and properties.

It is important to note that the accuracy and reliability of the BET method depend on proper instrument calibration, appropriate selection of the adsorbing gas, and careful data analysis. Following these steps diligently will ensure accurate surface area determination using the Brunauer-Emmett-Teller method.

## 4.2. Verification and interpretation of adsorption data

To measure gas adsorption, use convenient units and express the adsorbed gas amount in moles per gram of outgassed adsorbent. Specify the adsorbent's composition and characterize its surface properties if possible. For easy comparison, represent adsorption data graphically using adsorption isotherms. Plot the amount of gas adsorbed (preferably in  $\text{mol}\cdot\text{g}^{-1}$ ) against the equilibrium relative pressure ( $p/p_0$ ), where  $p_0$  is the saturation pressure of the pure adsorptive at the operating temperature. Alternatively, if the temperature exceeds the critical temperature of the adsorptive, plot the graph against absolute pressure  $p$ . For cases of significant deviation from ideality, particularly at high pressure, presenting the isotherms in terms of gas fugacity is preferred over pressure (Thommes *et al.*, 2015).

### 4.2.1. Classification of physisorption isotherms

An adsorption isotherm provides data on the maximum amount of adsorbate that a particular adsorbent can absorb at a specific pressure. To standardize experimental data for different "adsorbent-adsorbate" pairs, it is necessary to correlate them with various isotherm models. The International Union of Pure and Applied Chemistry (IUPAC) has classified adsorption pairs into eight different types based on the nature of the isotherms, as shown in **Figure 1**. The 77 K nitrogen adsorption-desorption isotherm is a commonly used method to assess the characteristics of porous materials. The nitrogen isotherms are typically acquired across the entire range of relative pressures ( $P/P_0$ ) from 0.00 to 0.99 (Aranovich & Donohue 1995; Xie *et al.*, 2004).

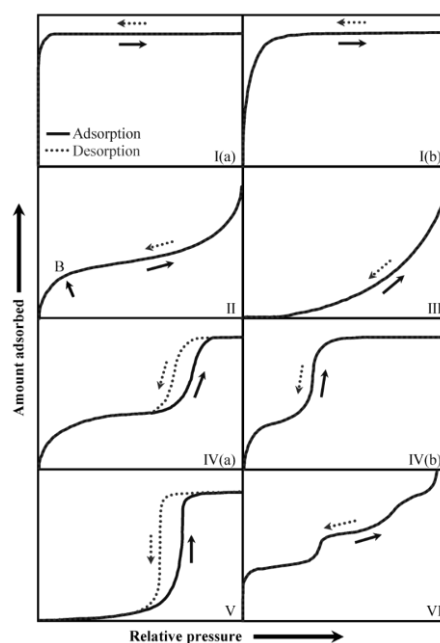


**Figure 1.** Physisorption isotherm classification adopted from Thommes *et al.* (2015).

Reversible Type I isotherms are observed in certain microporous solids with small external surfaces, such as activated carbons, molecular sieve zeolites, and specific porous oxides. The Type I isotherm is concave concerning the  $p/p_0$  axis, and the adsorbate amount reaches a maximum value. This maximum uptake is determined by the accessible micropore volume rather than the internal surface area. Strong adsorbent-adsorptive interactions in narrow micropores cause a steep uptake at very low  $p/p_0$ , leading to micropore filling at these low pressures. Type-I(a) isotherm is typical for narrow microporous adsorbents with a pore size of less than approximately 1 nm. Type-I(b) isotherms are found in materials with a broader distribution of pore sizes, including wider micropores and possibly narrow mesopores with widths less than about 2.5 nm.

Type-II isotherm also involves multilayer adsorption, closely resembling Type-I(b) but lacking the plateau. The uptake continuously increases, even when the pressure ratio is near unity. If the knee in the isotherm is sharp, it typically corresponds to the point (Point B) where monolayer coverage is completed, and the middle section becomes almost linear. A more gradual curvature (with a less distinctive Point B) indicates a significant overlap of monolayer coverage and the onset of multilayer adsorption. The thickness of the adsorbed multilayer tends to increase indefinitely as the relative pressure ( $p/p_0$ ) approaches 1.

The shape of Type-III adsorption isotherm is convex. The uptake remains low at low pressures but rises sharply at higher pressures. Unlike a Type II isotherm, the amount of adsorbate remains finite even at the saturation pressure (when  $p/p_0 = 1$ ).

Type-IV isotherm is categorized into Type-IV(a) and Type-IV(b), based on pore width. Type-IV(a) is observed in adsorbents with pore widths greater than 4 nm and displays hysteresis. On the other hand, Type-IV(b) is found in adsorbents with cylindrical and conical mesopores having widths smaller than 4 nm. Type-IV(b) exhibits complete reversibility, with closure at the tapered end. Initially, there is monolayer-multilayer adsorption on the mesopore walls, following a similar pattern as in a Type II isotherm. However, this is followed by pore condensation, where the gas condenses to a liquid-like phase in a pore at a pressure  $p$  lower than the saturation pressure  $p_0$  of the bulk liquid. A distinct characteristic of Type IV isotherms is a final saturation plateau, which may vary in length and could be reduced to a mere inflection point.

In the low  $p/p_0$  range, the Type V isotherm resembles Type III due to relatively weak adsorbent-adsorbate interactions. However, at higher  $p/p_0$ , molecular clustering occurs, followed by pore filling. Type V isotherms, for example, occur when water is adsorbed on hydrophobic microporous and mesoporous adsorbents. Type-V is known for its distinctive S-shaped isotherm and exhibits a hysteresis loop.

Type-VI isotherm represents adsorption occurring in distinct steps. This reversible stepwise isotherm is characteristic of layer-by-layer adsorption on a highly uniform nonporous surface. Each step's height indicates the capacity for the adsorbed layer, and the sharpness of the steps depends on the system and temperature. One of the best examples of Type VI isotherms is observed with argon or krypton at low temperatures on graphitized carbon blacks.

#### 4.2.2. Classification of physisorption isotherms

Hysteresis occurs when both adsorption and desorption reach saturation, but the desorption process does not follow the same path as the adsorption isotherm. This phenomenon is often linked to capillary condensation, which is responsible for filling and emptying mesopores. The presence of a hysteresis loop indicates the presence of distinct and controllable mesopores, and this is influenced by the shape and position of the isotherm



(Leofanti *et al.*, 1998). The types of hysteresis loops are represented by the IUPAC classification given in **Figure 2**.

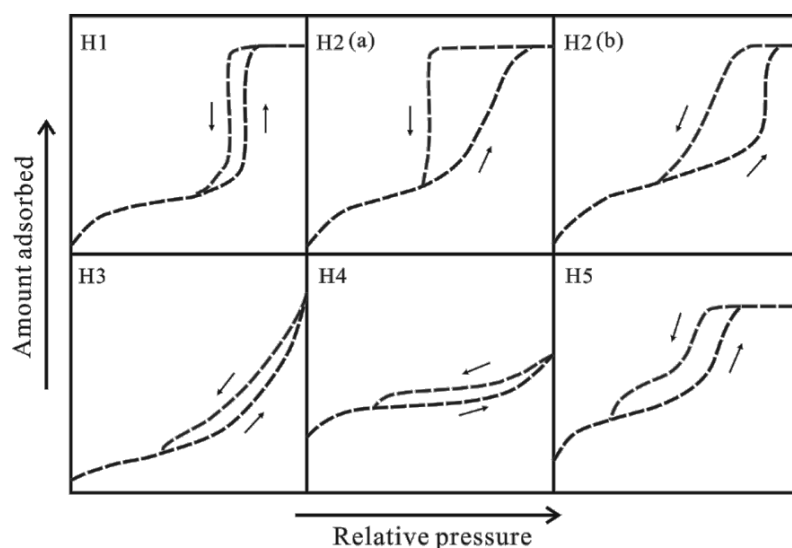


**Figure 2.** Classification of hysteresis loops adopted from [Thommes \*et al.\* \(2015\)](#).

Type H1 hysteresis loop is characteristic of porous materials with cylindrical or tubular pores having a narrow distribution of uniform pores. The adsorption-desorption isotherms are nearly parallel and vertical. The formation of a cylindrical meniscus during adsorption occurs at a higher relative pressure than the emptying process. Type H2 hysteresis loop features a large region with a long flat plateau and a steep desorption isotherm. This shape is associated with spheroidal cavities, voids, or "inkbottle" pores. The liquid trapped in the body of the pore is allowed to evaporate from the porous neck. However, the release of vapor condensation is limited due to the small radius of the porous neck. Type H3 hysteresis loop does not exhibit limiting adsorption at high relative pressure ( $p/p_0 = 0.09$ ). This is observed in nonrigid aggregates of plate-like particles, resulting in slit-shaped pores. Type H4 hysteresis loop is often associated with narrow slit-like pores and is related to type I isotherms in microporous materials.

Type H5 hysteresis loop is uncommon but exhibits a unique shape linked to specific pore structures containing open and partially blocked mesopores, such as plugged hexagonal templated silicas. The sharp step-down of the desorption branch is a common feature shared by H3, H4, and H5 loops. This step-down is typically observed within a narrow range of  $p/p_0$  for the specific adsorptive and temperature, for example, around  $p/p_0 \sim 0.4 - 0.5$  for nitrogen at 77 K. **Table 1** summarizes the physisorption isotherms and hysteresis loops of some materials.

**Table 1.** Isotherm and Hysteresis loops type.

Material	Physisorption Isotherm	Hysteresis Loops	Reference
Mudstone	Type IV(b)	Type H2(b)	<a href="#">(Lahn <i>et al.</i>, 2020)</a>
Silver doped hydroxyapatites	Type IV(b)	Type H3	<a href="#">(Chatterjee <i>et al.</i>, 2022)</a>
Magnesium hydroxide and oxide	Type III	Type H3	<a href="#">(Yu <i>et al.</i>, 2004)</a>
Titanium dioxide	Type IV(a)	Type H1	<a href="#">(Li <i>et al.</i>, 2019)</a>
ZSM-5 zeolites	Type I(a)	Type H4	<a href="#">(Liang <i>et al.</i>, 2021)</a>
Graphitic carbon nitride	Type II	Type H3	<a href="#">(Shang <i>et al.</i>, 2021)</a>
Carbon micropores	Type V	Type H2(a)	<a href="#">(Liu <i>et al.</i>, 2019)</a>

## 5. CONCLUSION

The Brunauer-Emmett-Teller (BET) method is a powerful tool for determining the specific surface area of inorganic materials, and our comprehensive guide has provided valuable insights into its application. Through a detailed exploration of the theoretical background, experimental procedures, and data analysis techniques, we have presented a systematic approach to accurately measuring the specific surface area of porous materials. It is essential to acknowledge the limitations and potential sources of errors in the BET method, which can arise due to assumptions, sample preparation, or instrumental factors. Careful attention to these aspects is critical for obtaining accurate and meaningful results. This guide is a valuable resource for researchers, providing them with the necessary knowledge and tools to apply the BET method effectively and make meaningful contributions to the study and development of inorganic materials.

## 6. ACKNOWLEDGMENT

The authors thank DIKTI for funding this research work (148/E5/PG.02.00.PL/2023) and DPRM through project number 3018/UN6.3.1/PT.00.2023. The facilities from Universitas Padjadjaran, Indonesia, and UIN Sunan Gunung Djati, through LITAPDIMAS number 5199/Un.05/V.2/TL.00/11/2022.

## 7. AUTHORS' NOTE

The authors declare that there is no conflict of interest regarding the publication of this article. Authors confirmed that the paper was free of plagiarism.

## 8. REFERENCES

- Aranovich, G. L., and Donohue, M. D. (1995). Adsorption isotherms for microporous adsorbents. *Carbon*, 33(10), 1369-1375.
- Brunauer, S., Emmett, P. H., and Teller, E. (1938). Adsorption of gases in multimolecular layers. *Journal of The American Chemical Society*, 60(2), 309-319.
- Chatterjee, T., Ghosh, M., Maji, M., Ghosh, M., Pradhan, S. K., and Meikap, A. K. (2022). Study of microstructural and electrical properties of silver substituted hydroxyapatite for drug delivery applications. *Materials Today Communications*, 31, 103360.
- Kruk, M., Jaroniec, M., and Sayari, A. (1997). Application of large pore MCM-41 molecular sieves to improve pore size analysis using nitrogen adsorption measurements. *Langmuir*, 13(23), 6267-6273.
- Lahn, L., Bertier, P., Seemann, T., and Stanjek, H. (2020). Distribution of sorbed water in the pore network of mudstones assessed from physisorption measurements. *Microporous and Mesoporous Materials*, 295, 109902.
- Leofanti, G., Padovan, M., Tozzola, G., and Venturelli, B. J. C. T. (1998). Surface area and pore texture of catalysts. *Catalysis Today*, 41(1-3), 207-219.
- Li, Y., Wang, W., Wang, F., Di, L., Yang, S., Zhu, S., Yao, Y., Ma, C., Dai, B., and Yu, F. (2019). Enhanced photocatalytic degradation of organic dyes via defect-rich TiO<sub>2</sub> prepared by dielectric barrier discharge plasma. *Nanomaterials*, 9(5), 720.



- Liang, G., Li, Y., Yang, C., Hu, X., Li, Q., and Zhao, W. (2021). Synthesis of ZSM-5 zeolites from biomass power plant ash for removal of ionic dyes from aqueous solution: equilibrium isotherm, kinetic and thermodynamic analysis. *RSC Advances*, *11*(36), 22365-22375.
- Liu, L., Zeng, Y., Tan, S. J., Xu, H., Do, D. D., Nicholson, D., and Liu, J. (2019). On the mechanism of water adsorption in carbon micropores—A molecular simulation study. *Chemical Engineering Journal*, *357*, 358-366.
- Mutolib, A., Rahmat, A., Triwisesa, E., Hidayat, H., Hariadi, H., Kurniawan, K., Sutiharni, S., and Sukanto, S. Biochar from agricultural waste for soil amendment candidate under different pyrolysis temperatures. *Indonesian Journal of Science and Technology*, *8*(2), 243-258.
- Nandiyanto, A. B. D., Fiandini, M., Fadiah, D. A., Muktakin, P. A., Ragadhita, R., Nugraha, W. C., Kurniawan, T., Bilad, M. R., Yunas, J., and Al Obaidi, A. S. M. (2023). Sustainable biochar carbon microparticles based on mangosteen peel as biosorbent for dye removal: Theoretical review, modelling, and adsorption isotherm characteristics. *Journal of Advanced Research in Fluid Mechanics and Thermal Sciences*, *105*(1), 41-58.
- Nandiyanto, A. B. D., Fiandini, M., Ragadhita, R., Maryanti, R., Al Husaeni, D. F., and Al Husaeni, D. N. (2023). Removal of curcumin dyes from aqueous solutions using carbon microparticles from jackfruit seeds by batch adsorption experiment. *Journal of Engineering Science and Technology*, *18*(1), 653-670.
- Nandiyanto, A. B. D., Fiandini, M., Ragadhita, R., Maryanti, R., Al Husaeni, D. F., and Al Husaeni, D. N. (2023). Removal of curcumin dyes from aqueous solutions using carbon microparticles from jackfruit seeds by batch adsorption experiment. *Journal of Engineering Science and Technology*, *18*(1), 653-670.
- Nandiyanto, A. B. D., Girsang, G. C. S., and Rizkia, R. S. (2022). Isotherm adsorption characteristics of 63-um calcium carbonate particles prepared from eggshells waste. *Journal of Engineering Science and Technology*, *17*, 3203-3210.
- Nandiyanto, A. B. D., Hofifah, S. N., and Ragadhita, R. (2022). Adsorption isotherm analysis of floating composite zinc imidazole framework-8 in millimeter epoxy cubes. *Journal of Engineering Science and Technology*, *17*(6), 4187-4202.
- Nandiyanto, A. B. D., Hofifah, S. N., Girsang, G. C. S., Trianadewi, D., Ainsiyifa, Z. N., Siswanto, A., Putri, S. R., Anggraeni, S., Maryanti, R., and Muslimin, Z. (2022). Distance learning innovation in teaching chemistry in vocational school using the concept of isotherm adsorption of carbon microparticles. *Journal of Technical Education and Training*, *14*(1), 14-26.
- Nandiyanto, A. B. D., Maharani, B. S., and Ragadhita, R. (2023). Calcium oxide nanoparticle production and its application as photocatalyst. *Journal of Advanced Research in Applied Sciences and Engineering Technology*, *30*(3), 168-181.
- Nandiyanto, A. B. D., Nur, N., and Taufik, R. S. R. (2022). Investigation of adsorption performance of calcium carbonate microparticles prepared from eggshells waste. *Journal of Engineering Science and Technology*, *17*(3), 1934-1943.
- Nandiyanto, A. B. D., Ragadhita, R., Fiandini, M., Maryanti, R., Al Husaeni, D. N., and Al Husaeni, D. F. (2023). Adsorption isotherm characteristics of calcium carbon

- microparticles prepared from chicken bone waste to support sustainable development goals (SDGS). *Journal of Engineering, Science and Technology*, 18(2), 1363-1379.
- Nasrollahzadeh, M., Atarod, M., Sajjadi, M., Sajadi, S. M., and Issaabadi, Z. (2019). Plant-mediated green synthesis of nanostructures: mechanisms, characterization, and applications. *Interface Science and Technology*, 28, 199-322.
- Odler, I. (2003). The BET-specific surface area of hydrated Portland cement and related materials. *Cement and Concrete Research*, 33(12), 2049-2056.
- Ragadhita, R., Amalliya, A., Nuryani, S., Fiandini, M., Nandiyanto, A. B. D., Hufad, A., Mudzakir, A., Nugraha, W. C., Farobie, O., Istadi, I., and Al-Obaidi, A. S. M. (2023). Sustainable carbon-based biosorbent particles from papaya seed waste: preparation and adsorption isotherm. *Moroccan Journal of Chemistry*, 11(2), 11-2.
- Ragadhita, R., and Nandiyanto, A. B. D. (2021). How to calculate adsorption isotherms of particles using two-parameter monolayer adsorption models and equations. *Indonesian Journal of Science and Technology*, 6(1), 205-234.
- Shang, Q., Fang, Y., Yin, X., and Kong, X. (2021). Structure modulation of gC 3 N 4 in TiO 2 {001}/gC 3 N 4 hetero-structures for boosting photocatalytic hydrogen evolution. *RSC Advances*, 11(59), 37089-37102.
- Shimizu, S., and Matubayasi, N. (2022). Surface Area Estimation: Replacing the Brunauer–Emmett–Teller Model with the Statistical Thermodynamic Fluctuation Theory. *Langmuir*, 38(26), 7989-8002.
- Thomas, K. M. (2023). Perspectives of Gas Adsorption and Storage in Kerogens and Shales. *Energy and Fuels*, 37(4), 2569-2585.
- Thommes, M., Kaneko, K., Neimark, A. V., Olivier, J. P., Rodriguez-Reinoso, F., Rouquerol, J., and Sing, K. S. (2015a). Physisorption of gases, with special reference to the evaluation of surface area and pore size distribution (IUPAC Technical Report). *Pure and Applied Chemistry*, 87(9-10), 1051-1069.
- Xie, J., Wang, X., and Deng, J. (2004). Modifying the pore structure of Pit-ACF with the chemical vapor deposition of methane and propylene. *Microporous and Mesoporous Materials*, 76(1-3), 167-175.
- Yang, S., Cheng, Q., Hu, L., Gu, Y., Wang, Y., and Liu, Z. (2023). Study on the adsorption properties of oxalic acid-modified cordierite honeycomb ceramics for neutral red dyes. *ACS Omega*, 8(12), 11457-11466.
- Yu, J. C., Xu, A., Zhang, L., Song, R., and Wu, L. (2004). Synthesis and characterization of porous magnesium hydroxide and oxide nanoplates. *The Journal of Physical Chemistry B*, 108(1), 64-70.